Highlights on Spanish Astrophysics X, Proceedings of the XIII Scientific Meeting of the Spanish Astronomical Society held on July 16 – 20, 2018, in Salamanca, Spain. B. Montesinos, A. Asensio Ramos, F. Buitrago, R. Schödel, E. Villaver, S. Pérez-Hoyos, I. Ordóñez-Etxeberria (eds.), 2019

Angular Redshift Fluctuations. A New Cosmological Observable.

Carlos Hernández-Monteagudo[1]

[1] Centro de Estudios de Física del Cosmos de Aragón (CEFCA)
Plaza San Juan, 1, E-44001, Teruel, Spain

Abstract

We study the angular statistical properties of maps of galaxy redshifts as computed as the average weighted redshift of all galaxies falling in the same sky pixel. The choice for this weights is a Gaussian centered upon some input redshift $z_{\rm obs}$ and with a typical width σ_z in the range 10^{-2}–10^{-1}. At each position of the sky $\hat{n}$, this defines an angular map of redshifts given by $z(\hat{n}) = \bar{z} + \delta z(\hat{n})$. We predict the angular power spectrum of such angular redshift fluctuations (ARF), for every generic choice of $z_{\rm obs}$ and σ_z, under cosmological linear perturbation theory. We find that ARF are sensitive to the underlying cosmological density and radial peculiar velocity fields, providing a *tomographic* description of those fields which does not rely upon any fiducial cosmological model converting redshifts into distances. The ARF are also found to provide *additional* cosmological information on top of that provided by angular galaxy density fluctuations (ADF), while behaving much more robustly in the presence of systematics biasing the observed number of galaxies. These theoretical predictions are confirmed when comparing to the outcome of 100 COLA numerical simulations, which also quantify the impact of non-linear evolution at different angular scales and cosmological epochs. When applying our formalism on the BOSS DR12 spectroscopic galaxy sample, we obtain unprecedented tomographic and very competitive measurements on the galaxy bias and growth rate for the LOWZ and CMASS galaxy samples.

1 Introduction

For the last twenty years different efforts have been scanning the universe wider and deeper, attempting to gain insight on the processes of the expansion of the universe and the growth of structure therein [2, 11, 1, 5]. These processes encode precious information of the (arguably) largest enigmas in current fundamental physics: the nature of dark matter and dark energy. According to the standard cosmological model, the former is the dominant form of matter in the universe (about 5 times more abundance than standard, baryonic matter), while the latter constitutes a repulsive form of energy amounting to roughly 70 % of the total energy budget in the universe [9].

These two problems are, at the same time, coupled to other open questions in physics: is Einstein's theory of gravity correct on the largest cosmological scales? How much room is there left for alternative theories of gravity? What is the weight and hierarchy of the neutrinos? Are there other light particle species in the universe? Can we test extensions of the particle physics standard model with astrophysical and/or cosmological observations?

In this very exciting context, it becomes essential to develop techniques that assure an unbiased and quasi-optimal extraction of cosmological information out of the data. Currently, standard techniques compute the 2- and 3-point statistics of the spatial and/or angular density of galaxies, which are seen as biased samplers of the underlying matter density field. Since the only proxy for the distance to those galaxies is the observed redshift, it is customary to map the galaxies' angular and redshift coordinates into the tridimensional space. This process, however, requires the assumption of an underlying cosmological (fiducial) model that enables the mapping between the (observed) redshift and the corresponding distance to the galaxies. In this mapping, the contribution of the galaxies' radial peculiar motion becomes visible through the so-called *redshift space distortions* (RSD). These peculiar velocities are triggered by gravity, and thus provide information on the growth of structure at each cosmological epoch. Measuring these velocities accurately has implications not only for gravity, but also for dark energy studies and investigations towards the presence of additional light particle species in the universe.

Here we introduce a novel method to probe the cosmological density and radial peculiar velocity fields that (i) works in a tomographic way, providing a measurement for each choice of cosmological redshift, (ii) does not rely upon the assumption of any fiducial cosmological model, and (iii) is particularly robust with respect to systematics biasing the observed number density of matter tracers (galaxies, QSOs, etc).

2 The Angular Redshift Fluctuations (ARF)

The ARF are based upon the estimation of the average redshift, within a given sky pixel, of all galaxies falling in that pixel after assigning them a Gaussian weight. Such Gaussian weights are adopted to be of the form $W_j \equiv \exp -(z_j - z_{\rm obs})^2/(2\sigma_z^2)$, where z_j is the observed redshift of the j-th galaxy, and $z_{\rm obs}$ and σ_z are the observer's choices for the central redshift and redshift width with which conducting the analyses. In this way, for a given sky position/sky pixel $\hat{n}$, the ARF would be computed as

$$\delta z(\hat{n}) = \frac{\sum_{j\in\hat{n}} W_j (z_j - \bar{z})}{\langle \sum_{j\in\hat{n}} W_j \rangle_{\hat{n}}}. \quad (1)$$

The sum in the numerator goes through all galaxies falling within a pixel centred upon $\hat{n}$, and $\bar{z}$ stands for the average redshift of the sample under the same Gaussian width in the entire footprint of the survey, $\bar{z} = (\sum_j W_j z_j)/(\sum_j W_j)$. Finally, the brackets $\langle ... \rangle_{\hat{n}}$ denote angular averages over the same footprint of the galaxy survey.

As shown in [6], it is easy to show that, at first order, the ARF field is sensitive to both the matter density and the radial peculiar velocity fields under the Gaussian redshift

windows:

$$\bar{z}+\delta z(\hat{\mathrm{n}}) = \mathcal{F}[z_H]+\mathcal{F}[b_g\delta_{\mathrm{m}}\,(z_H-\mathcal{F}[z_H])]+\mathcal{F}\left[\frac{\mathbf{v}\cdot\hat{\mathrm{n}}}{c}(1+z_H)\left(1-\frac{d\log W}{dz}(z_H-\mathcal{F}[z_H])\right)\right]+\mathcal{O}(2^{\mathrm{nd}}), \tag{2}$$

where $\mathcal{F}[g]$ denotes the (normalized) integral of function g under the Gaussian redshift window, b_g refers to the galaxy bias, z_H is the Hubble flow redshift, and $\mathbf{v}$ is the proper peculiar velocity vector.

The kernels are such if either the matter density δ_m or the line-of-sight velocity are constant under the Gaussian window, then they do not contribute to the ARF: for δ_m, the kernel is very close to a line-of-sight dipole/gradient, while for the line-of-sight velocity the kernel is sensitive to smaller scale radial variations. Interestingly, for small values of σ_z (σ_z 10^{-2}), these kernels are practically orthogonal to the corresponding kernels of the galaxy number angular density fluctuations (hereafter ADF), that are given by

$$\delta_g(\hat{n}) = \mathcal{F}[b_g\delta_{\mathrm{m}}\,] + \mathcal{F}\left[\frac{\mathbf{v}\cdot\hat{\mathrm{n}}}{c}(1+z_H)\frac{d\log W}{dz}\right] + \mathcal{O}(2^{\mathrm{nd}}). \tag{3}$$

This means that the ARF provide *complementary* information to that provided by ADF. Furthermore, it is also worth mentioning that, due to the peculiar gradient-like form of the kernel for the δ_m term, the ARF are highly correlated to the line-of-sight projected peculiar velocities under the Gaussian redshift shell, making the ARF an ideal proxy for radial peculiar velocities at any redshift. This permits cross-correlating ARF maps with other maps containing information about radial peculiar velocities, like CMB maps containing contribution from the kinetic Sunyaev-Zeldovich effect (see [4] for first application of this methodology on CMB data from the *Planck* experiment).

Finally, if at the time of conducting any given galaxy survey the observed number of galaxies in a given region of the sky is biased due to either multiplicative (γ) or additive (ϵ) systematics, $n_{g,\mathrm{obs}} = \gamma(n_g + \epsilon)$, then it is easy to prove that the resulting ARF will be biased only by the additive systematics if these change significantly under the (usually narrow) redshift Gaussian window shell, $\delta z_{\mathrm{obs}} = \delta z + \mathcal{F}[\epsilon(z - \bar{z})]$. Otherwise, the impact of systematics biasing the ADF cancels at leading order for the ARF.

3 Comparison to numerical simulations

In order to asses the correctness of the equations outlined in the previous section, we compare those equations with the output of 100 *quick* numerical simulations computed with the `COLA` algorithm [8]. These simulations were run on a 3 Gpc box, with 1024^3 particles under a set of cosmological parameters compatible to *Planck* observations [9], see [3] for further details. For each of these simulations, a lightcone providing the position and peculiar velocity for each particle was computed, and the resulting comparison is shown in Fig. 1. In the left set of panels in Fig. 1 we provide the raw comparison of the average of the angular power spectra (C_ls) from the COLA simulations (solid lines in top panels) with the linear theory expectations (dashed lines). This comparison is conducted at $z_{\mathrm{obs}} = 0.5$ and $\sigma_z = 0.01$.

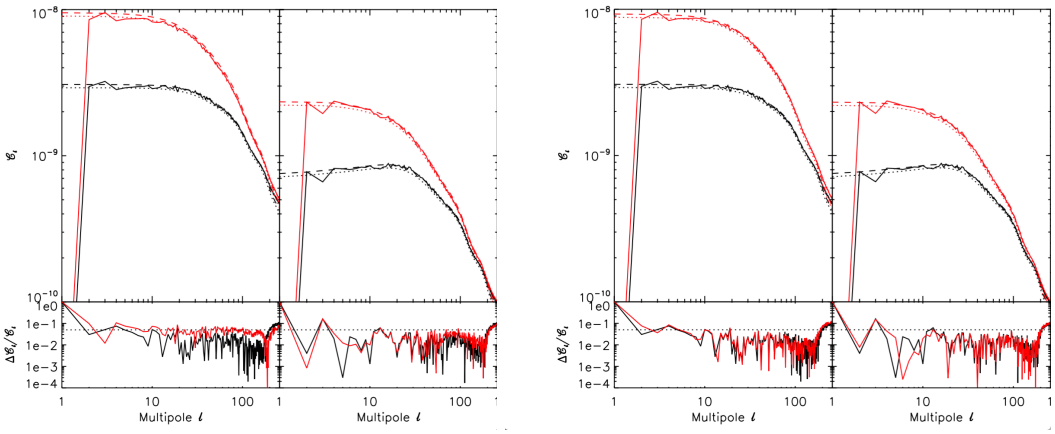

Figure 1: *Left set of panels:* Comparison of measured angular power spectra C_ls from theory and COLA simulations. The left panels refer to ARF, while the right panels to ADF. Bottom panels display relative errors. Black and red colors refer to real and redshift space, respectively. This comparison is conducted for a Gaussian redshift shell centered upon $z_{\rm obs} = 0.5$ and width $\sigma_z = 0.01$. *Right set of panels:* Comparison of measured angular power spectra C_ls as in the left set of panels, but after introducing a correction for non-linear velocities as a thermal, Gaussian PDF of $\sigma_{th} = 1\,500\,{\rm km\,s^{-1}}$.

The dotted lines display the linear theory expectations suppressed by 5 %. Red color denote results obtained in redshift space (i.e., the selection of the particles under the Gaussian redshift window takes into account the particles' peculiar velocities), while the black lines are obtained in real space, after nulling the particles' peculiar velocities. In both plots, the left panels refer to ARF angular power spectra, while the right panels to the angular power spectra of ADF. We can see that, in the left two panels of Fig. 1, the comparison of the angular power spectra in real space (black color) is very good: the bottom panels (providing the relative error) show that differences between the theory and the average output of the simulations is at the level of a few percent, as expected from the number of COLA simulations. In redshift space, however, the situation is different: the velocities seem to drive the C_ls for ARF systematically below the linear theory expectation by $\sim 5\,\%$. This low bias is not so evident for ADF, and is absent for wider choices of σ_z, $\sigma_z > 0.02$, and higher values of $z_{\rm obs}$.

It turns out that this low bias is due to non-linear, thermal peculiar velocities of the particles in the simulations, caused by non-linear gravitational growth of structures, affecting preferentially small spatial scales and later epochs/lower redshifts. This can be easily modeled by a Gaussian distribution function of the type $\mathcal{P} \propto \exp -v_{los}^2/(2\sigma_{th}^2)$, with the value of the thermal broadening in the radial velocity distribution function being a fit from numerical simulations. In the right set of panels in Fig. 1 we show that adopting $\sigma_{th} = 1\,500\,{\rm km\,s^{-1}}$ provides a satisfactory fit in all multipoles up to $l \sim 150$, where the impact of other non-linearities become dominant. The value of $\sigma_{th} = 1\,500\,{\rm km\,s^{-1}}$ is indeed higher than expected for typical thermal motions of particles at $z_{\rm obs} = 0.5$. This effective value of thermal broadening also includes the smearing of anisotropy due to the fact that galaxies/particles are

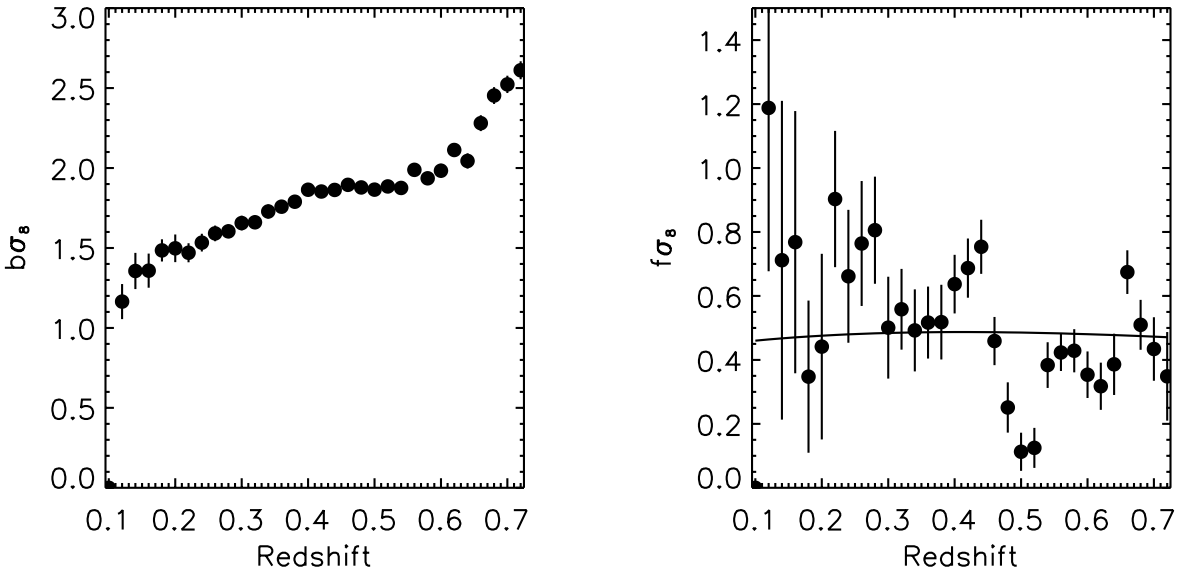

Figure 2: Preliminary measurements of the bias and growth rate for the LOWZ and CMASS galaxy samples of Data Release 12.

selected in redshift space: for a finite particle number density, the selection of particles under the Gaussian redshift modifies the anisotropy pattern, and this (un-modeled) effect is more important for narrow redshift shells.

4 First application to real data and conclusions

We use the Data Release 12 of the BOSS collaboration for testing the proposed methodology. In particular, we focus on both the LOWZ and CMASS galaxy samples, which contain more than 1.2 million galaxies in a footprint covering almost a quarter of the sky ($f_{sky} \approx 0.23$). We compute both the ADF and the ARF, but find that the former, on the large angular scales, are dominated by spurious power that is known to be caused predominantly by the blinding induced by stars at the moment of target definition (see, e.g., [10], for one of the first works addressing systematics in BOSS data). We see that the ARF are, instead, pretty immune to these systematics, and find no clear evidence for excess power. These confirms our expectations that ARF are more robust against systematics, as outlined above.

We conduct ARF tomography throughout the redshift range sampled by the LOWZ and CMASS samples, providing measurements of the galaxy bias $b_g\sigma_8$ and the velocity growth factor $f\sigma_8$ after combining our measurements with those of the *Planck* experiment. We display our results in Fig. 2, which is obtained after combining the information for ARF measurements with $\sigma_z = 0.01$ and 0.05. Our bias and velocity measurements are compatible

with previous estimates of the BOSS collaboration, although ours constitute the first tomographic estimations with unprecedented redshift resolution. We are currently polishing these measurements, and exploring the possibility of constraining dark energy and the nature of gravity with these data (see [7] for further details).

The ARF constitute a new cosmological observable which is sensitive to both the density and radial velocity fields. It works in a tomographic way, its phases are correlated to those of the projected radial velocities, and is particularly robust against systematics biasing the observed number density of galaxies. Its application on real data is currently providing competitive measurements of the growth rate of the universe. Future prospects for this observable include (but are not limited to) measurements of f_{NL}, the parameter accounting for local-type non-Gaussianity during inflation, the presence of light particle species, relativistic corrections (including gravitational potential shifts), or its application in Lyman-α or in HI 21 cm surveys.

Acknowledgments

I thank the SEA SOC for giving me the opsportunity of presenting this work during the SEA Scientific Meeting at the University of Salamanca, my *Alma mater*.

References

[1] Alam, S., Ata, M., Bailey, S., et al. 2017, MNRAS, 470, 2617

[2] Colless, M., Dalton, G., Maddox, S., et al. 2001, MNRAS, 328, 1039

[3] Chaves-Montero, J., Angulo, R. E., & Hernández-Monteagudo, C. 2018, MNRAS, 477, 3892

[4] Chaves-Montero, J., Hernández-Monteagudo, C., Hurier, G., & Angulo, R. E., 2018, MNRAS (in preparation)

[5] Dawson, K. S., Kneib, J.-P., Percival, W. J., et al. 2016, AJ, 151, 44

[6] Hernández-Monteagudo, C., Hurier, G., Chaves-Montero, J., Angulo, R., & Bonoli, S., 2017, Physical Review Letters, (submitted).

[7] Hernández-Monteagudo, C., Hurier, G., Chaves-Montero, J., Angulo, R., Aricò, G., & Bonoli, S., 2018, Physical Review Letters, (in preparation).

[8] Koda, J., Blake, C., Beutler, F., Kazin, E., & Marin, F. 2016, MNRAS, 459, 2118

[9] Planck Collaboration, Ade, P. A. R., Aghanim, N., et al. 2016, A&A, 594, A13

[10] Ross, A. J., Ho, S., Cuesta, A. J., et al. 2011, MNRAS, 417, 1350

[11] Wakamatsu, K., Colless, M., Jarrett, T., et al. 2003, The Proceedings of the IAU 8th Asian-Pacific Regional Meeting, Volume 1, 289, 97